2,2′-Thiodiethanol: A New Water Soluble Mounting Medium for High Resolution Optical Microscopy

THORSTEN STAUDT,[1,2] MARION C. LANG,[1] REBECCA MEDDA,[2]
JOHANN ENGELHARDT,[1] AND STEFAN W. HELL[1,2]*
[1]*German Cancer Research Center Heidelberg, High Resolution Optical Microscopy Division, Heidelberg, Germany*
[2]*Department of Nanobiophotonics, Max Planck Institute for Biophysical Chemistry, Göttingen, Germany*

KEY WORDS imaging; fluorescence; refractive index mismatch; aberration

ABSTRACT The use of high numerical aperture immersion lenses in optical microscopy is compromised by spherical aberrations induced by the refractive index mismatch between the immersion system and the embedding medium of the sample. Especially when imaging >10 μm deep into the specimen, the refractive index mismatch results in a noticeable loss of image brightness and resolution. A solution to this problem is to adapt the index of the embedding medium to that of the immersion system. Unfortunately, not many mounting media are known that are both index tunable as well as compatible with fluorescence imaging. Here we introduce a nontoxic embedding medium, 2,2′-thiodiethanol (TDE), which, by being miscible with water at any ratio, allows fine adjustment of the average refractive index of the sample ranging from that of water (1.33) to that of immersion oil (1.52). TDE thus enables high resolution imaging deep inside fixed specimens with objective lenses of the highest available aperture angles and has the potential to render glycerol embedding redundant. The refractive index changes due to larger cellular structures, such as nuclei, are largely compensated. Additionally, as an antioxidant, TDE preserves the fluorescence quantum yield of most of the fluorophores. We present the optical and chemical properties of this new medium as well as its application to a variety of differently stained cells and cellular substructures. *Microsc. Res. Tech. 70:1–9, 2007.*

INTRODUCTION

Diffraction theory dictates that the lateral width of the main maximum of the point spread function (PSF) of a lens decreases linearly in size with its numerical aperture (NA); along the optical axis (z) the decrease is even quadratic. Since the NA is given by $n \sin \alpha$, optical microscopy has struggled to accomodate semiaperture angles α and refractive indices n to be as large as possible. Because of the relatively large n that is close to that of glass coverslips (1.515), optical-grade oil has become the standard immersion liquid for high aperture lenses and, by the same token, oil immersion lenses have become the gold standard for high resolution optical microscopy. The glass–oil immersion system offers a well-matched, optically homogenous system that yields a focal spot that is ideally only limited by diffraction. Unfortunately, the situation deteriorates if the converging spherical wavefronts are focused into a sample with a different index of refraction, such as a sample that is mounted in a glycerol-based medium (n = 1.43–1.47) or into a sample that is kept in an aqueous buffer. In this case, the focal spot is blurred due to the spherical aberrations resulting from the mismatch in n (Hell et al., 1993).

The problems arising from mismatched n are prevalent both in conventional and confocal microscopy (Pawley, 1995), but in the latter they are clearly manifested as a loss of image brightness and as poorer optical sectioning (Egner et al., 1998; Hell et al., 1993). Therefore, in the last decade, most microscope manufacturers have developed high aperture water immersion lenses of NA = 1.2, i.e., $\alpha = 64^\circ$, that are essential for the 3D high resolution imaging of live cells.

To account for the fact that most fixed cells are mounted in glycerol-based media, coverslip corrected glycerol immersion lenses have also been developed. Featuring an angle of $\alpha = 68.5^\circ$, the most sophisticated version of these lenses (NA = 1.35) enable the nearly aberration-free high resolution imaging of glycerol mounted samples (Martini et al., 2002), in the conventional, confocal, as well as in the 4Pi mode (Gugel et al., 2004). However, besides being expensive, a limitation of the NA = 1.35 glycerol lenses is that they require the use of fused silica coverslips of nonstandard thickness and glycerol as an immersion medium. A common way to increase the refractive index in an aqueous mounting medium is to add proteins such as bovine serum albumine or glucose (Müller, 1956). However, the adjustable range of the refractive index is here limited from 1.33 to about 1.43.

In this paper, we report an alternative solution to the refractive index mismatch problem: a novel mounting medium whose refractive index can be continuously tuned between that of water and that of immersion oil. This solution is not only cost-effective but also enables a flexible use of all immersion lenses available, includ-

*Correspondence to: Prof. Stefan W. Hell, High Resolution Optical Microscopy Division, German Cancer Research Center Heidelberg, Im Neuenheimer Feld 280, 69120 Heidelberg, Germany. E-mail: hell@4pi.de

Received 9 October 2006; accepted in revised form 20 October 2006

DOI 10.1002/jemt.20396

Published online 27 November 2006 in Wiley InterScience (www.interscience.wiley.com).

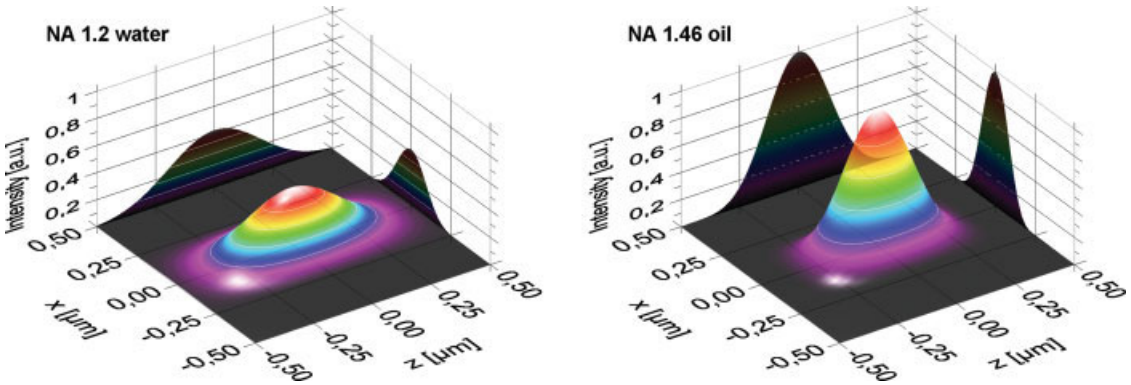

Fig. 1. Surface plots of an axial section (xz) of the main maximum of the PSF of a confocal microscope for a water immersion lens with NA = 1.2 (**left**) and an oil immersion lens with NA = 1.46 (**right**); excitation, 488 nm; emission, 525 nm. The PSF of the oil immersion lens is narrower by 30% along the z-axis. Additionally, the 30% larger collection and excitation efficiency results in a doubled peak intensity.

ing the novel oil immersion lenses of ultrahigh aperture angle, $\alpha = 75^\circ$.

Increasing the NA by increasing the aperture angle as well as the refractive index of the mounting medium pays off in many regards. For example, water immersion lenses with NA = 1.2, i.e., $\alpha = 64^\circ$, have a 40% poorer axial resolution as compared to the 1.46 oil immersion lenses featuring $\alpha = 75^\circ$ (Fig. 1). The larger α of the latter also brings about a 30% larger fluorescence collection. However, a simple consideration based on geometrical optics shows that if the n of the mounting medium departs by 0.001, the marginal rays at $\alpha = 75^\circ$ already miss the focal point by about the wavelength of light, at a sample depth of 30 µm. This departure is four times smaller at $\alpha = 59^\circ$ of a 1.3 NA oil immersion objective. This simple example illustrates the importance of refractive index matching when high angle lenses are to be employed.

Therefore, the use of high angle lenses calls for an embedding medium whose refractive index can be precisely controlled. Ideally, it is miscible with water at any concentration, nontoxic, and easily applicable to biological samples. It should quickly immerse all the structures without destroying or deforming them and must not quench the fluorescence notably.

MATERIALS AND METHODS

Medium

For preparation, 2,2′-thiodiethanol (TDE) (CAS 111-48-8, highest purity, No. 88559 Sigma-Aldrich) is adjusted to a pH of 7.5 with 1.2 M hydrochloric acid. About 970 µL TDE mixed with 30 µL 1×PBS (or other aqueous buffer solution) give 1 mL mounting medium with a refractive index of 1.515 and a pH value of 7.5 ± 1.

Buffers

The water amount in the final solution contains physiological buffer solution (PBS) which consists of 137 mM NaCl, 2.68 mM KCl, 8 mM Na_2HPO_4, and 1.47 mM KH_2PO_4; pH = 7.5.

Cell Culture and Immunocytochemistry

PtK2 cells were grown as described previously (Osborn et al., 1977). For immunocytochemistry, the cells were seeded on standard glass coverslips to a confluency of 50–80% and permeabilized with cold methanol (−20°C) for 4–6 min. The cells were subsequently washed in PBS with 1% BSA (blocking buffer) and incubated with primary antibodies (anti α-tubulin rabbit IgG, 1 µg/mL, Abcam, Cambridge, UK; anti-β-tubulin mouse IgG, 1 µg/mL, Sigma-Aldrich; anti-β-actin mouse IgG, 1 µg/mL, Sigma-Aldrich; anti-α-subunit of F_1F_0-ATP-synthase mouse IgG, 1 µg/mL, Molecular Probes, Carlsbad, CA). After 1 h of incubation, the cells were washed with blocking buffer for 10 min and incubated with secondary antibodies (Alexa 488 goat anti-rabbit IgG, 10 µg/mL, Molecular Probes, Carlsbad, CA; Alexa 546 goat anti-mouse IgG, 10 µg/mL, Molecular Probes, Carlsbad, CA; Cy5-conjugated sheep anti-mouse IgG, 15 µg/mL, Dianova, Hamburg, Germany; Cy3-conjugated sheep anti-mouse IgG, 15 µg/mL, Dianova, Hamburg, Germany; DY-485XL-conjugated sheep anti-mouse IgG, 15 µg/mL, Dyomics GmbH, Jena, Germany) for 1 h. Nucleus staining was performed by incubating cells 15–30 min in the presence of DAPI (dissolved in ethanol 2 µg/mL, Sigma). For imaging, the cells were mounted in 97% TDE containing 0.02 M phosphate buffer of pH 7.5.

Cell Transfection

For staining the matrix, cells were transiently transfected with GFP and DsRed, respectively, fused to a mitochondrial targeting sequence. Cells were grown to a confluency of about 80%, trypsinized, washed, and resuspended in transfection buffer (120 mM KCl, 10 mM KH_2PO_4, 10 mM K_2HPO_4, 2 mM EGTA, 5 mM $MgCl_2$, 25 mM HEPES, 0.15 mM $CaCl_2$, 5 mM GSH, 2 mM ATP) containing 10 µg of DNA (pcDNA3.1(+)-preSu9 (1-69)-GFP and pDsRed1-Mito, Clontech). A double-pulse protocol was used for electroporation (GenePulser, d = 2 mm, U = 800 V, R = 200 W, C = 25 µF, BioRad) and cells were seeded on glass coverslips. Around 12–16 h after transfection they were fixed in 3.7% formaldehyde and mounted in 97% TDE.

Imaging

For imaging, we used a confocal microscope TCS SP2 (Leica Microsystems, Mannheim, Germany) equipped with immersion micro-objectives 63 × 1.2 NA W CORR

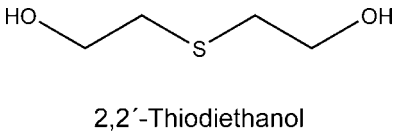

Fig. 2. TDE (2,2′-thiodiethanol) is a nontoxic glycol derivative which, owing to the sulfur atom, exhibits a large polarizability and hence a high refractive index. It is soluble in water at any concentration.

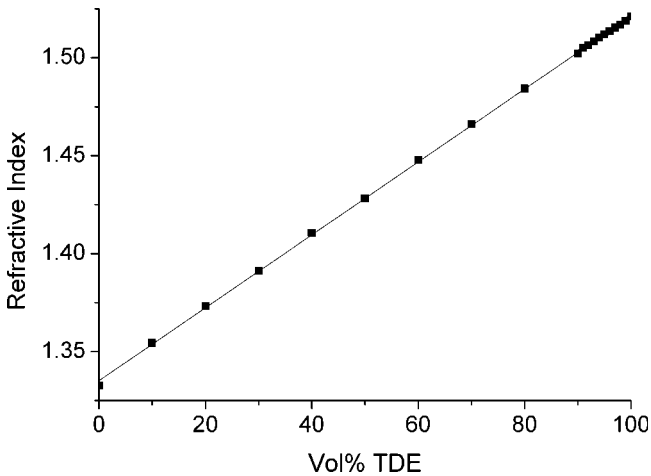

Fig. 3. TDE (2,2′-thiodiethanol) is miscible with water in any proportion. The refractive index of the solution can be precisely tuned to any value between 1.333 (water) and 1.521. The latter is even slightly larger than that of immersion oil.

for the reference samples in buffer and 63 × 1.4 NA Oil or 100 × 1.4 NA Oil for imaging of the samples in TDE, respectively. Phase contrast images were taken with a DMRE microscope (Leica Microsystems, Mannheim, Germany) equipped with digital camera D10 (Canon, Japan) and objective N PLAN L 40 × 0.55 NA CORR PH2.

Fluorescence Dyes

The following dyes were used for the spectroscopic measurements: coumarine 120 (Lambda Physik, Göttingen, Germany), coumarine 153 (Lambda Physik, Göttingen, Germany), fluorescein isothiocyanate (Isomer I) (FITC) (No. F1906, Molecular Probes, Carlsbad), Oregon Green® 488 (No. Q6142, Molecular Probes, Carlsbad), Texas Red® (No. T1905, Molecular Probes, Carlsbad), BODIPY® FL, SE (No. D2184, Molecular Probes, Carlsbad), BODIPY® 650/665-X, SE (No. D-10001, Molecular Probes, Carlsbad), Cy3 NHS (No. PA13101, Amersham Biosciences, Buckinghamshire, UK), A532 NHS (No. AD 532-3, Atto-Tec, Siegen, Germany), A565 NHS (No. AD 565-3, Atto-Tec, Siegen, Germany), A655 NHS (No. AD 655-3, Atto-Tec, Siegen, Germany), EGFP, mRFP.

Spectra

The transmission spectrum was measured with a Cary 500 scan spectrometer (Varian, Darmstadt, Germany) in a semi micro cell (Hellma, Müllheim, Germany). Fluorescence spectra were recorded with a Cary eclipse fluorescence spectrophotometer (Varian, Darmstadt, Germany). Absorption spectra were measured with a Cary 4000 UV–VIS spectrophotometer (Varian, Darmstadt, Germany).

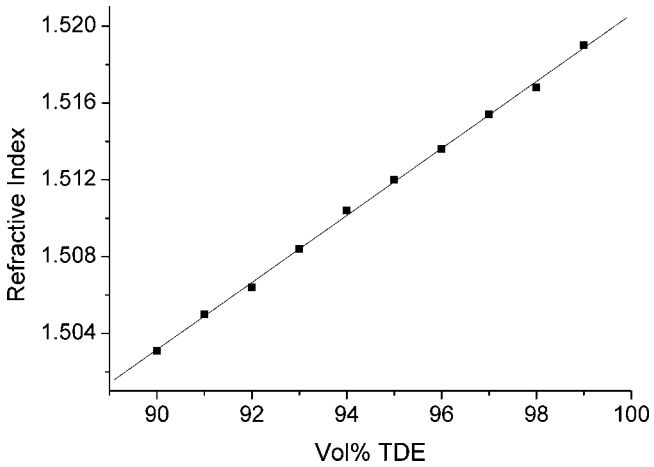

Fig. 4. TDE allows a precise setting of the refractive index by adjusting the water content. For use with an oil immersion lens, a TDE concentration of 97% in water was employed.

Refractive Index

The refractive index of the mounting medium was measured with an AR200 digital hand-held refractometer (Reichert, NY) as a n_D^{23} value (refractive index at 589 nm and 23°C). The refractive index of a standard immersion oil is typically specified as $n_e = 1.518$ (refractive index at 546 nm).

Dispersion Measurements

The beam of an Innova 70 Ar/Kr-Ion-Laser (Coherent, Santa Clara) was separated spectrally using a prism and coupled into a model 197 Abbe refractometer (Carl Zeiss, Jena, Germany). The refractive index was measured at 466, 476, 483, 488, 514, 521, 531, 568, and 647 nm to determine the dispersion of TDE.

Temperature Dependence

The Abbe refractometer was connected to a thermostat to measure the refractive index dependence on the temperature of TDE.

pH-Measurement

The pH value of the mounting medium was controlled by a PT-10 pH-Meter (Sartorius, Göttingen, Germany) equipped with a PY-P22 electrode (Sartorius, Göttingen, Germany).

Preparation

At first, the staining and fixation of cells was performed as in conventional or confocal fluorescence microscopy. When using TDE in biological samples, one must consider that (1) by adding an adequate buffer (for example, pH 8) the pH is set to the value required for optimum performance of the used dye. (2) An exchange of water with TDE (97% for oil immersion) must be slow enough to prevent cell shrinkage due to osmotic shock (TDE enters the cell or nucleus slower

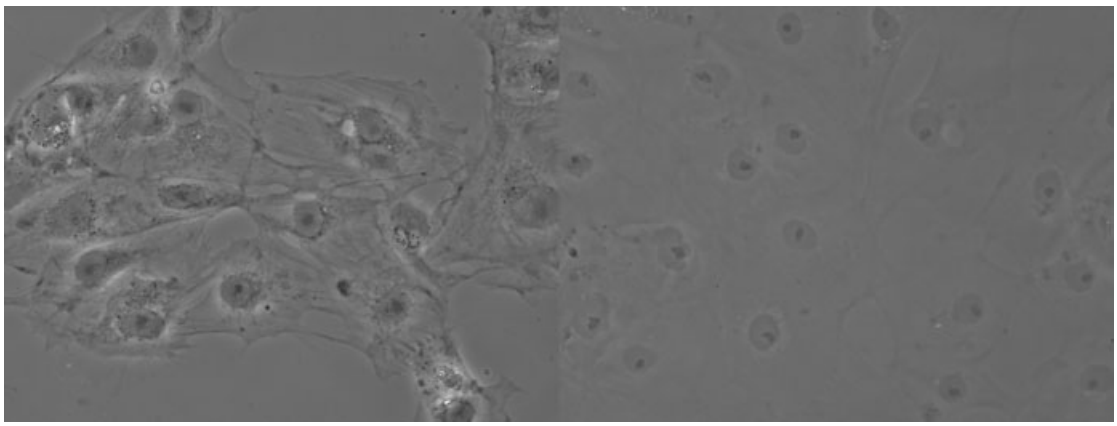

Fig. 5. Phase contrast images of PtK2 cells. **Left**: Cells mounted in buffer solution. **Right**: Cells mounted in 97% TDE solution. As expected, the contrast generated by local refractive index changes is greatly reduced in TDE.

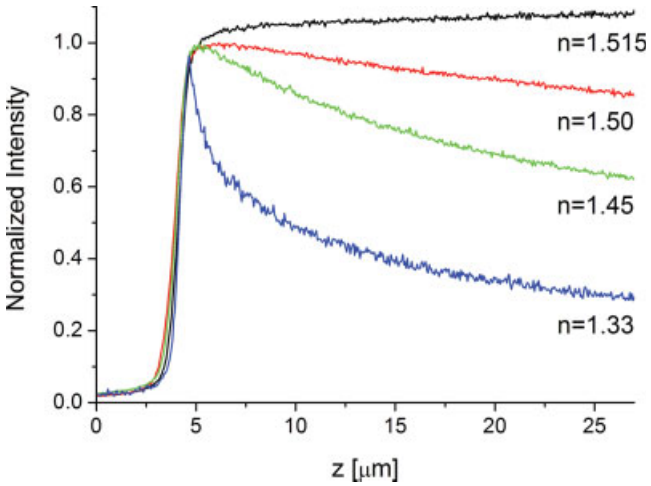

Fig. 6. Confocal axial (z-) scans at the interface of a dye solution with the glass coverslip using an oil immersion lens of 1.46 NA, $\alpha = 75^{\circ}$. The coverslip is located at $z = 4.0$ μm. At positions $z < 4$ μm is glass and dye solution at $z > 4$ μm. The curves correspond to four different refractive indices set by using different TDE concentrations, as indicated. The deeper the beam is focused into the sample, the fewer photons are collected due to spherical abberations introduced by refractive index mismatch. In case of matching refractive index the signal is constant along the optic axis.

than water leaves it due to their different permeabilities).

Mounting Procedure

After fixation of the cells and depending on the sample, various dilutions with increasing TDE content were used to exchange the water with TDE in a continuous or stepwise manner. Good results have been obtained with the following steps:

- 10% TDE (100 μL TDE, 50 μL PBS5×, 850 μL water),
- 25% TDE (250 μL TDE, 50 μL PBS5×, 700 μL water),
- 50% TDE (500 μL TDE, 50 μL PBS5×, 450 μL water), and then three times
- 97% TDE (970 μL TDE, 30 μL PBS1×).

The samples were successively immersed in the above solutions with increasing TDE concentrations for about 5–10 min each. Then the coverslips of the samples were sealed with nail polish. The refractive index of the solution was examined with a refractometer. The pH value of all stock solutions was controlled by a pH meter. Because of the viscosity of TDE, it is important to allow for a few minutes for the settling to the final measurement value. At the microscope, the correction collar of the objective lens was adjusted to maximum fluorescence brightness. This corrects for residual spherical aberrations due to temperature or coverslip thickness mismatches. To observe potential quenching effects of TDE, micromolar dye solutions in TDE were examined in a Varian fluorescence spectrometer.

RESULTS

In order to identify mounting media with the proper refractive index, we screened the properties of 12,000 substances with regard to refractive index, solubility in water, pH value, toxicity, and stability (Weast, 1974). TDE, a glycol derivative, was identified as a very promising candidate (Fig. 2). Used as an antioxidant for the chromatography of amino acids (Moore and Stein, 1951), TDE is an inexpensive and almost odorless chemical. It is classified as being irritating but nontoxic. Further, mounting media candidates are also to be found among the organic iodides, sulfides (thioles), and aromatic compounds featuring strongly polarizable groups. However, toxicity, reactivity, and low solubility in water may limit the number of useful ones. Therefore, we have limited our study to TDE.

The data in Figure 3 show that adjusting the amount of water in TDE allows a precise control of the refractive index of the medium. Therefore, it is possible to tune the refractive index of the sample to that of the immersion oil.

The precision of the refractive index tuning is further evidenced in Figure 4, showing the range around 1.51 in detail. A 97% TDE volume yields a refractive index which perfectly matches that of immersion oil at room temperature. By the same token, it is possible to

TABLE 1. Absorption (Abs.) and fluorescence intensities (Em.) of dye solutions in PBS buffer and TDE (97%) were measured as well as the wavelengths λ of the absorption and emission maxima

	PBS (Ref.)				TDE					
	Abs.	λ_{Abs} (nm)	Em. (a. u.)	λ_{Em} (nm)	Abs.	λ_{Abs} (nm)	Em. (a. u.)	λ_{Em} (nm)	Rel. QY	
Coumarines										
Coumarine 120	0.092	342	580	444	0.119	342	315	438	0.42	
Coumarine 153	0.029	434	75	550	0.055	434	348	539	2.45	
Rhodamines										
FITC Isomer I	0.135	495	812	518	0.154	505	560	532	0.60	
Oregon Green 488	0.047	493	800	518	0.057	506	595	530	0.61	
Texas Red mixed Iso.	0.025	586	820	605	0.027	590	830	607	0.94	
A565 NHS	0.031	567	210	586	0.049	567	460	589	1.39	
A532 NHS	0.027	532	317	550	0.034	542	240	559	0.60	
Oxazines										
A655 NHS	0.039	661	590	676	0.051	666	720	686	0.93	
Cyanines										
Cy3	0.037	551	135	563	0.036	563	595	576	4.53	
Boradiazaindacenes										
Bodipy 650/665-x	—	—	—	—	0.072	662	900	677	—	1*
Bodipy FL-SE	0.016	502	536	510	0.030	510	488	518	0.49	
Fluor. proteins										
EGFP	0.008	489	277	520	0.014	490	343	510	0.71	2*
mRFP	0.081	586	505	606	0.088	587	467	608	0.85	

To compare the effective fluorescence behavior of the dyes in TDE with PBS buffer, the ratio $QY_{rel} = \frac{Em_{TDE}}{Em_{PBS}} \cdot \frac{Abs_{PBS}}{Abs_{TDE}}$ is shown in the last column. Values > 1 indicate stronger fluorescence in TDE. (1* Bodipy is quenched in buffer due to dimerisation; 2* in 80% TDE).

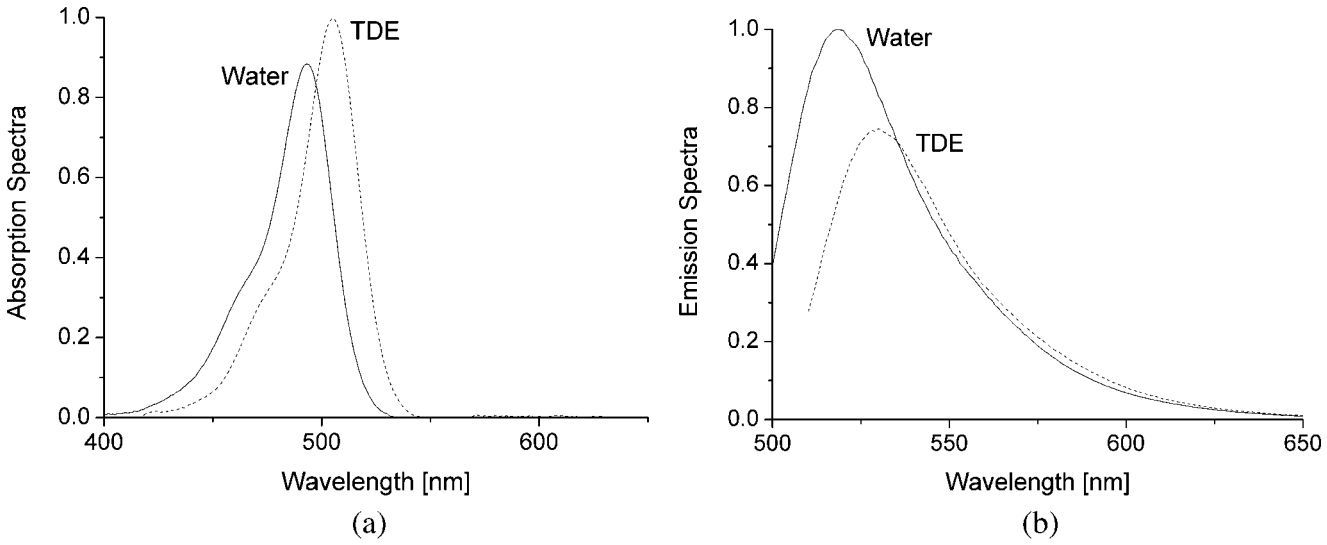

Fig. 7. Comparison of the absorption and emission spectra of Oregon Green 488 in water and in 97% TDE. The spectra are red shifted by 12 nm.

match the refractive index for different ambient temperatures.

Another important feature of TDE is that its dispersion matches the dispersion of regular immersion oil (see appendix); hence no additional chromatic aberration is induced. As expected, embedding cells in a 97% TDE solution significantly reduces the phase contrast which demonstrates the improvement of the optical properties of fixed samples for high resolution imaging (Fig. 5).

The effect of spherical aberrations caused by refractive index mismatch in the mounting medium is easily measured by evaluating an *xz*-scan of a homogeneous dye solution in a confocal microscope. We recorded such an *xz*-scan using a 100× NA 1.46 oil immersion lens featuring $\alpha = 75^{\circ}$. The fluorophore rhodamine 6 G was dissolved in PBS buffer containing different amounts of TDE to set certain refractive indices in the mounting medium. Figure 6 (left) shows the measured intensity along the optical axis. The intensity drops quickly after a few μm in depth if the refractive index does not match that of the immersion system. The loss of resolution and intensity in depth is most dramatic at $n = 1.33$ (water) and $n = 1.45$ corresponding to 20/80 water/glycerol solution. But there is still a significant effect at $n = 1.50$ which is closer to glass than polymer mounted samples such as polymethyl methacrylate (PMMA) or Mowiol ($n = 1.49$). Evidently, only the correct setting of the refractive index at $n = 1.515$ at 97% TDE avoids aberrations in the sample and optimizes the fluorescence collection.

TDE is hygroscopic; this must be taken into account during preparation and for handling the stock solutions. Additional physical properties are summarized in the appendix.

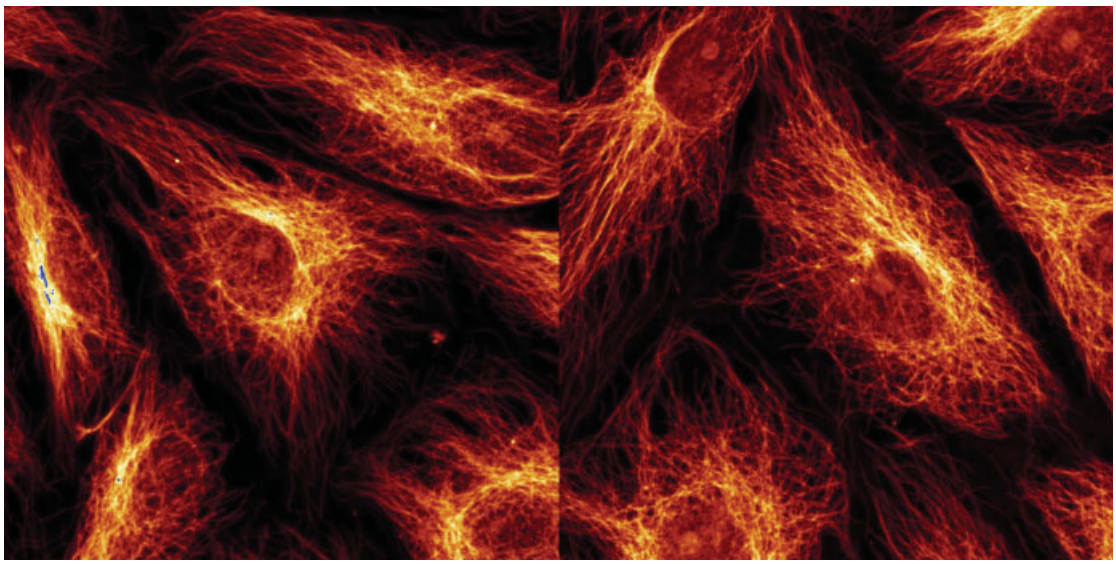

Fig. 8. PtK2 cells with immunolabeled microtubules mounted in PBS (**left**) and in 97% TDE (**right**) demonstrate the viability of TDE as an embedding medium. Immunolabeling with the fluorophore Dyomics-485XL. No structural difference or substantial difference in image brightness is observed.

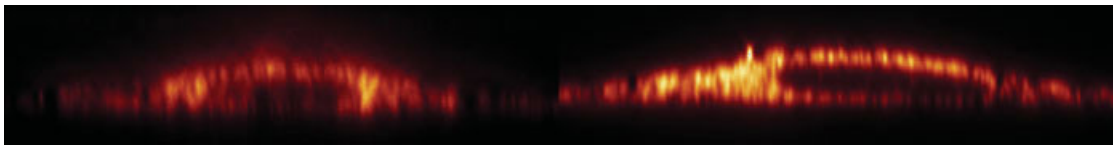

Fig. 9. PtK2 cells as in Figure 7; confocal *xz*-sections show the conservation of the 3D structure in 97% TDE.

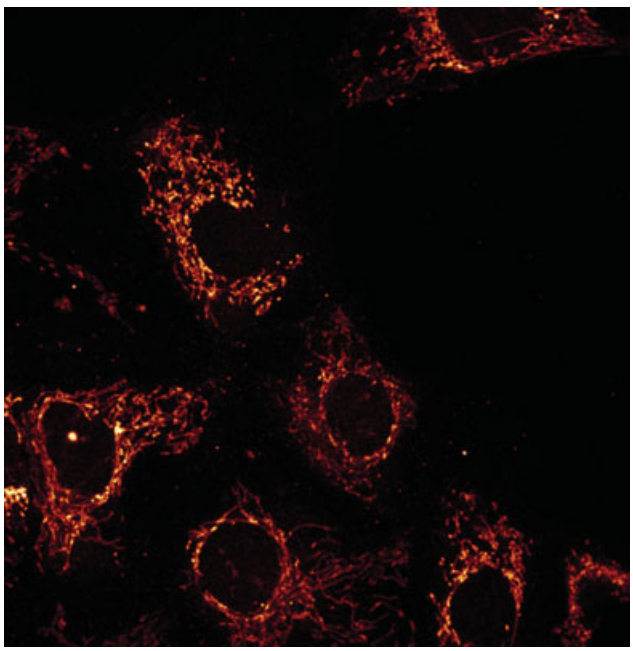

Fig. 10. PtK2 cells in 97% TDE. ATP-synthase immunostained with Alexa 546.

To provide an overview about the general applicability and behavior of popular classes of dyes, the fluorescence efficiencies of dyes have been measured in PBS and TDE using a fluorescence spectrometer. The results are summarized in Table 1 showing the relative absorption (Abs), emission (Em), and quantum yields of the dyes as defined by $\mathrm{QY}_{\mathrm{rel}} = \frac{\mathrm{Em}_{\mathrm{TDE}}}{\mathrm{Em}_{\mathrm{PBS}}} \cdot \frac{\mathrm{Abs}_{\mathrm{PBS}}}{\mathrm{Abs}_{\mathrm{TDE}}}$. The table allows a quick and practical comparison of the fluorescence yields of the dyes mounted in TDE or PBS. We selected representative derivatives of coumarines, rhodamines, oxazines, cyanines, and boradiazaindacenes. In addition, we also investigated the behavior of fluorescent proteins and quantum dots.

The data shows that in some cases the fluorescence brightness is slightly lower in TDE as compared to PBS. However, in practical microscopy, this minor effect is usually compensated by the larger collection efficiency of the high NA lens. Nevertheless, also the opposite effect, i.e., stronger fluorescence is observed in a number of cases.

We also found that the absorption and emission spectra are slightly altered by the mounting medium, which is a quite common phenomenon when dye molecules are embedded into media with different polarizability. The absorption spectra also appear slightly redshifted in accordance with Kundt's rule and other related effects (LeRosen and Reid, 1952). Figure 7 gives an example with the commonly used fluorescent marker Oregon Green 488. The excitation and emission filters of the microscopes may therefore require

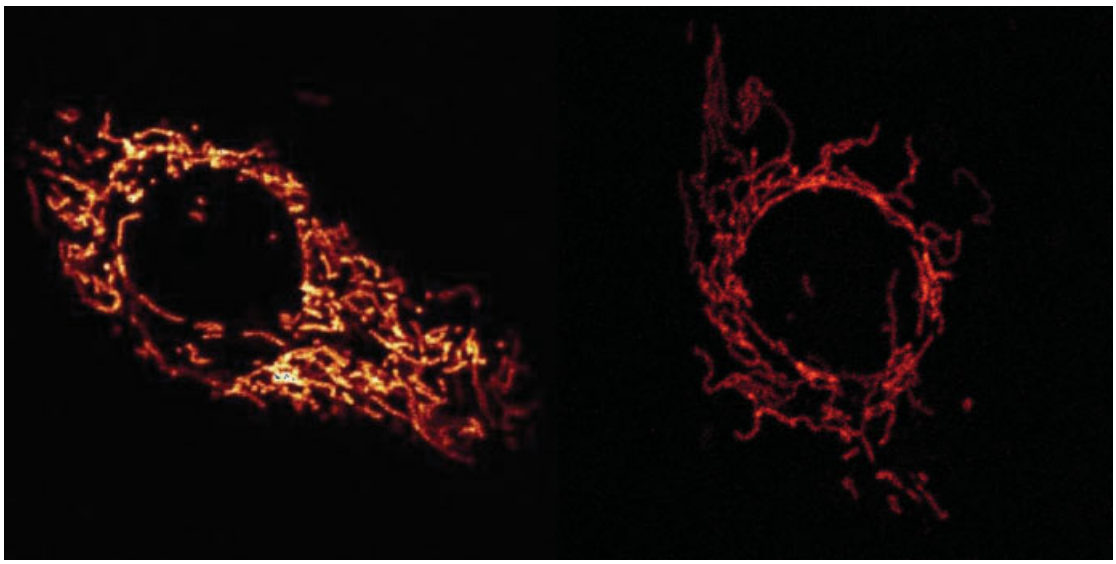

Fig. 11. **Left**: PtK2 cell in 97% TDE: mitochondrial matrix stained with DsRed. **Right**: PtK2 cell in 85% TDE: mitochondrial matrix stained with EGFP.

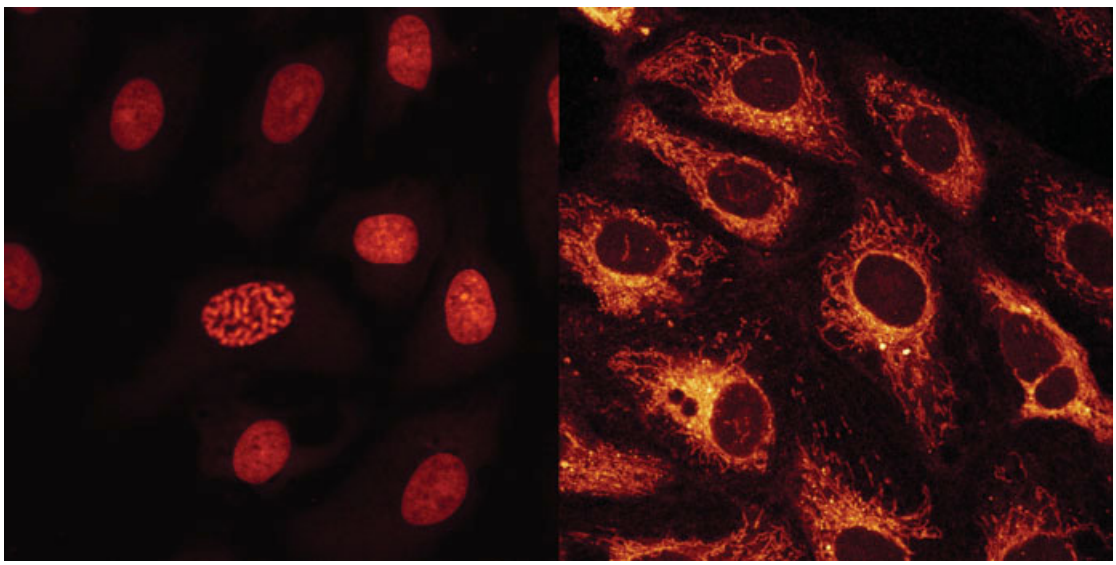

Fig. 12. PtK2 cells embedded in 97% TDE. **Left**: DAPI staining of nuclei. **Right**: Mitochondria stained with DIOC6.

slight adaptations. On the other hand, no significant differences have been observed when using different buffers such as PBS, HEPES, TRIS, or HBS-buffer for index adjustment of the TDE based medium.

Cell membranes are permeable for TDE; hence permeabilization with detergents such as Triton X-100 is not required. Virtually, all standard procedures of labeling with exogenous fluorophores, such as immunostaining or chromatine labeling with DAPI worked flawlessly. As the only exception, phalloidin conjugated fluorophores used to stain the actin cytoskeleton have been destabilized in TDE. A remedy may be a strong postfixation after phalloidin incubation.

Interestingly, we found that the brightness of fluorescent proteins (FP) increases with increasing fraction of TDE in the medium up to a certain TDE concentration. We have prepared mammalian cells (PtK2) in which the enhanced green fluorescent protein (EGFP) was fused to a mitochondrial matrix targeting sequence. We found that EGFP was quenched if the TDE fraction was >80–85%. In contrast, the fluorescence of the monomeric red fluorescent protein (mRFP) is not affected by high TDE concentrations. At a 97% TDE concentration ($n = 1.515$), mRFP performs virtually as in PBS. Hence, while it seems to be difficult to match EGFP mounted fixed samples to a refractive index $n > 1.48$, it is possible to embed mRFP labeled samples in a strongly concentrated TDE based medium with large refractive index. Semiconductor quantum dots and fluorescent beads performed in the TDE-based solution at all TDE concentrations.

We also observed that some dyes, e.g., Cy3 and Coumarine 153, displayed increased brightness while other dyes became dimmer in TDE as compared to PBS. Interestingly, Cy3 emitted >4 times more intensely in TDE, which may be attributed to the arresting of this photoisomerizable molecule in the fluorescent transstate of the cis–trans system (Heilemann et al., 2005; Widengren and Schwille, 2000).

The general applicability of TDE as a mounting medium for fluorescence imaging is exemplified in Figures 8–12. We also note that TDE has a slightly smaller temperature coefficient than regular oil immersion fluid. The temperature dependence of TDE is shown in the appendix.

DISCUSSION AND CONCLUSION

Used as an embedding medium, TDE allows a precise adjustment of the refractive index. This feature is an important prerequisite for biological microscopy of fixed samples at the largest possible aperture angle. The refractive index can be readily adjusted using a refractometer. The resulting new $n = 1.515$ medium consisting of 97% TDE and 3% PBS or similar buffers is compatible with many cell preparation and staining methods.

The investigation of TDE in the bulk shows weak autofluorescence around 430 and 570 nm for excitation at 350 and 510 nm, respectively. However, the autofluorescence is so low that it is hardly noticeable in conventional fluorescence microscopy applications; we regard it as irrelevant in confocal recordings.

Unless the exchange process is too fast, the replacement of water by TDE does not disturb the 3D structure of the cell. Water can obviously penetrate cellular or nuclear membranes much faster than TDE, but this can be easily accounted for by a stepwise or continuous solution exchange, as described in the methods section. The usefulness of TDE is further supported by the fact that immunostaining and DNA staining using DAPI is possible, as well as the imaging with quantum dots and FP. The only exception with regard to applicability is that, unlike the fluorescence of mRFP, that of EGFP is quenched for TDE concentrations larger than 80%, that is for refractive indices > 1.48. This observation might give further hints to the fluorescence properties of EGFP and will be investigated in the future.

The observed spectral shifts by a few nanometers are in accordance with the fact that the change in fluorophore-solvent interactions influences the electronic transitions of the fluorophore. For the same reason, the fluorescence quantum yield of a number of dyes is slightly modulated. However, in most cases, these changes are surprisingly subtle and do not compromise the usefulness of TDE as a mounting medium. Last but not least, the reducing property of TDE helps to reduce photobleaching.

Another interesting application could be the use of TDE as an immersion fluid. The unavoidable change of the refractive index in the immersion oil can be compensated in TDE by adjusting the proper concentration. Of course it must be ensured that the last optical element of the objective lens is not harmed by the TDE based medium.

In conclusion, the new mounting medium TDE is suitable for high resolution imaging of fixed specimens using objective lenses with the highest angles available. The refractive index in the sample can be adjusted from 1.334 (water) to 1.521 (beyond that of immersion oil) by adjusting the concentration of TDE to the required value. Unlike glycerol-based mounting media, TDE allows one to employ high angle oil immersion lenses of >68° semiaperture angle without compromising image formation by refractive index induced spherical aberration. The benefits are deeper sample penetration, an increase in the image brightness, and better resolution.

A further important benefit is the improved spatial invariance of the effective PSF of the conventional or confocal microscope which is particularly important for increasing the resolution by image deconvolution (Holmes et al., 1995). Last but not least, since the coherent use of opposing high angle spherical wavefronts is the essential physical ingredient in 4Pi and I^5M microscopy, we anticipate index matching by TDE to substantially advance the optical performance of these axially superresolving techniques.

ACKNOWLEDGMENTS

We acknowledge Sylvia Löbermann of the Max Planck Institute for Biophysical Chemistry for providing biological samples and Jaydev Jethwa for critical reading of the manuscript. We also thank the Institute of Physical Chemistry of the University of Heidelberg for the possibility to record transmission spectra of TDE.

APPENDIX: PHYSICAL PROPERTIES OF TDE

The dispersion of TDE (97% + 3% PBS buffer) is similar to that of the immersion medium. Hence, TDE does not induce chromatic aberrations in multicolor imaging or when imaging fluorophores with a large stokes shift (Fig. A1). The temperature dependence of the refractive index is displayed in Figure A2, showing that TDE features a rather moderate temperature dependence.

The optical absorption of TDE in the visible range is low and can be neglected for all microscopy applications. This is evidenced in Figure A3, showing the optical transmission through a 10 mm thick layer of TDE.

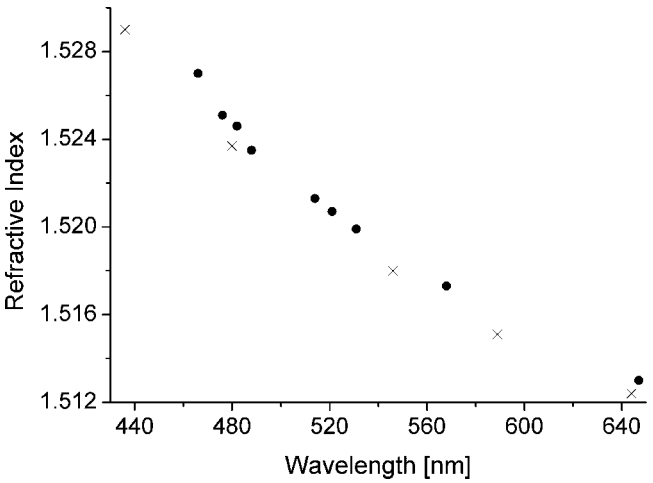

Fig. A1. The dispersion of TDE (dot) is close to the dispersion of standard immersion oil (Leica Microsystems) (cross). This avoids the chromatic aberrations otherwise introduced by the mounting medium.

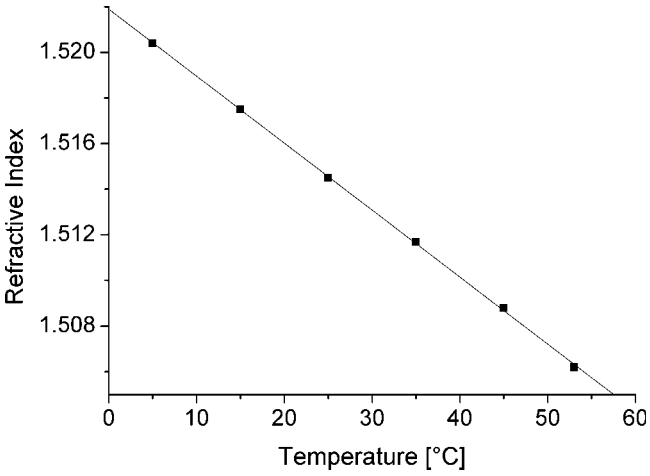

Fig. A2. The temperature dependence of the refractive index of TDE (3×10^{-4}/°C) is slightly less than that of the immersion oil (3.8×10^{-4}/°C).

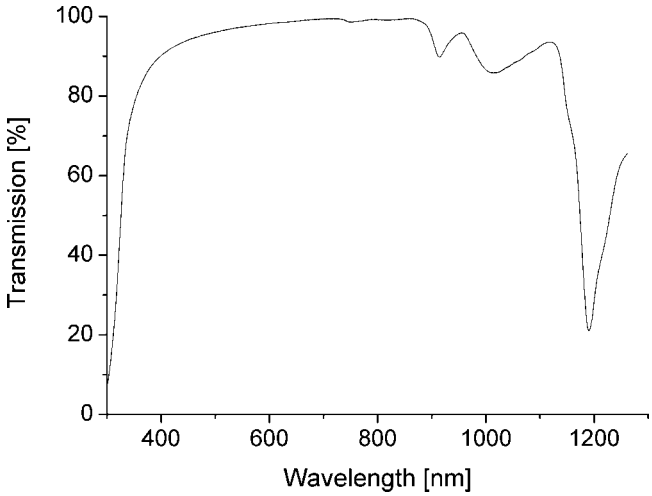

Fig. A3. The transmission spectrum of TDE (10 mm thickness) shows minimal absorption over the entire visible and near infrared range. For a microscope sample of 100 μm thickness, the transmission in the 360–1,100 nm spectral range is >99%.

REFERENCES

Egner A, Schrader M, Hell SW. 1998. Refractive index mismatch induced intensity and phase variations in fluorescence confocal, multiphoton and 4Pi-microscopy. Opt Commun 153:211–217.

Gugel H, Bewersdorf J, Jakobs S, Engelhardt J, Storz R, Hell SW. 2004. Cooperative 4Pi excitation and detection yields 7-fold sharper optical sections in live cell microscopy. Biophys J 87:4146–4152.

Heilemann M, Margeat E, Kasper R, Sauer M, Tinnefeld P. 2005. Carbocyanine dyes as efficient reversible single-molecule optical switch. J Am Chem Soc 127:3801–3806.

Hell S, Reiner G, Cremer C, Stelzer EHK. 1993. Aberrations in confocal fluorescence microscopy induced by mismatches in refractive index. J Microsc 169:391–405.

Holmes TJ, Bhattacharyya S, Cooper JA, Hanzel D, Krishnamurthi V, Lin W, Roysam B, Szarowski DH, Turner JN. 1995. Light microscopic images reconstruction by maximum likelihood deconvolution. In: Pawley J, editor. Handbook of biological confocal microscopy. New York: Plenum. pp. 389–400.

LeRosen AL, Reid CE. 1952 An investigation of certain solvent effect in absorption spectra. J Chem Phys 20:233–236.

Martini N, Bewersdorf J, Hell SW. 2002. A new high-aperture glycerol immersion objective lens and its application to 3D-fluorescence microscopy. J Microsc 206:146–151.

Moore S, Stein WH. 1951. Chromatography of amino acids on sulfonated polystyrene resins. J Biol Chem 192:663–681.

Müller R. 1956. Zur Verbesserung der Phasenkontrast-Mikroskopie durch Verwendung von Medien optimaler Brechungsindices. Mikroskopie 11:36–46.

Osborn M, Franke WW, Weber K. 1977. Visualization of a system of filaments 7–10 nm thick in cultured-cells of an epithelioid line (Pt K2) by immunofluorescence microscopy. Proc Natl Acad Sci USA 74:2490–2494.

Pawley J, editor. 1995. Handbook of biological confocal microscopy. New York: Plenum.

Weast RC. 1974. Handbook of chemistry and physics. Cleveland: CRC.

Widengren J, Schwille P. 2000. Characterization of photoinduced isomerization and back-isomerization of cyaninie dye Cy5 by fluorescence correlation spectroscopy. J Phys Chem A 104:6416–6428.